# ADAPTIVE SUPERVISORY CONTROL STRATEGY INTEGRATING FUZZY-LQR/LQI FOR UNMANNED SURFACE VEHICLES (USVs) UNDER VARYING ENVIRONMENTAL DISTURBANCES

**Le Quyet Thang[1,*], Tran Xuan Thuy[1], Tran Ngan Ha[1]**

DOI: https://doi.org/10.57001/huih5804.2026.103

**ABSTRACT**

Motion control for Unmanned Surface Vehicles (USVs) inherently faces a critical trade-off between energy optimization and robust operation under complex environmental disturbances. This paper proposes a hybrid Supervisory Control strategy that seamlessly integrates a Linear Quadratic Regulator (LQR) and Fuzzy Logic to address this challenge. The system architecture consists of a high-level Supervisor capable of classifying operating conditions to activate two distinct modes: (1) An Energy-Saving Mode employing a nominal LQR controller under calm sea conditions; and (2) An Adaptive Mode utilizing a Fuzzy- Linear Quadratic Integral (Fuzzy-LQI) controller with an anti-windup mechanism to eliminate steady-state errors under extreme weather conditions. Simulation results on the Cybership II model demonstrate that the proposed strategy not only significantly reduces energy consumption compared to conventional robust controllers but also maintains high tracking accuracy (error $< 0.2$m) despite strong wind and current disturbances.

***Keywords:*** *USV, LQR, Fuzzy Logic, Supervisory Control, Adaptive Control, Energy Optimization.*

[1]Quang Ninh University of Industry, Vietnam
[*]Email: lequyetthang5282@qui.edu.vn

Received: 01/3/2026
Revised: 15/4/2026
Accepted: 29/5/2026

## 1. INTRODUCTION

### 1.1. Background and Research Necessity

Hydrographic surveying is vital for managing Vietnam's extensive inland waterways and coastlines [1]. Due to the high operational costs and safety risks associated with traditional manned vessels [2], Unmanned Surface Vehicles (USVs) have emerged as an efficient alternative. However, compact USVs are highly susceptible to environmental disturbances (e.g., currents, waves, wind), which cause significant cross-track errors and excessive battery consumption due to continuous course corrections [3]. While traditional Proportional-Integral-Derivative (PID) controllers are widely used, they fail to eliminate steady-state errors under constant current disturbances [4]. Although the Linear Quadratic Regulator (LQR) offers an optimal balance between tracking error and control energy, standard LQR with fixed weighting matrices lacks the adaptability required for varying environments. Consequently, this paper proposes an Adaptive Fuzzy-LQI control architecture to overcome these limitations and provide a foundation for high-precision autonomous surveying.

### 1.2. Literature Review

Globally, USV control has shifted from classical methods to intelligent algorithms. Early studies predominantly utilized PID controllers [4]; however, Fossen [5] highlighted that PID approaches suffer from sluggish transient responses and fail to eliminate steady-state errors under constant marine disturbances. Advanced nonlinear strategies, such as Neural Networks and Sliding Mode Control (SMC) proposed by Wang and Pan [6], significantly improve tracking accuracy but impose heavy computational burdens and struggle with energy optimization. Alternatively, the standard LQR efficiently balances tracking and energy but inherently yields non-zero steady-state errors under constant ocean currents [7].

In Vietnam, USV research has primarily focused on mechanical design, such as composite hull optimization [8], or system integration like RF-controlled waste collection models [9]. Regarding control algorithms, most domestic studies still rely on traditional PID or Fuzzy-PID

controllers [10]. Therefore, the integration of optimal control with integral action (LQI) and Fuzzy Logic to achieve high-precision, energy-efficient path following remains a significant research gap.

### 1.3. Research Objectives and Contributions

This study aims to develop a robust path-following control strategy for USVs in bathymetric missions, ensuring high tracking precision under complex hydrodynamic disturbances. The primary contributions are:

**Hybrid Fuzzy-LQI Architecture:** The standard LQR framework is augmented with an integral action (LQI) to completely eliminate steady-state errors induced by persistent wind and currents, preventing vehicle drift during data acquisition.

Fuzzy Logic-Based Adaptive Mechanism: A Fuzzy Inference System (FIS) is utilized to dynamically tune the weighting matrices (*Q* and *R*) in real-time. This allows the USV to react aggressively to large deviations while maintaining smooth, energy-efficient motion when stabilized.

Dynamic Simulation Validation: The proposed strategy is validated in a Python-based simulation environment using a 3-DOF nonlinear USV model with stochastic environmental disturbances. Comparative results demonstrate the proposed controller's superiority over the standard LQR in both minimizing tracking errors and optimizing actuator energy consumption.

## 2. USV DYNAMIC MODELING AND ENVIRONMENTAL DISTURBANCES

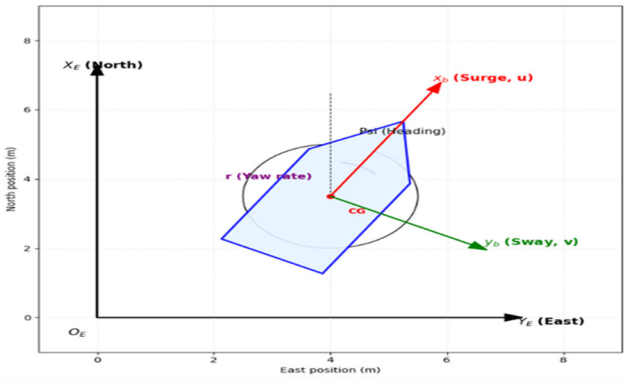


Figure 1. Illustration of the reference coordinate systems and the three degrees of freedom (Surge, Sway, Yaw) of the USV

To facilitate the design of a high-precision trajectory tracking controller, the formulation of a mathematical model that accurately captures the hydrodynamic behavior of the USV is a fundamental prerequisite. In this study, a 3-Degrees-of-Freedom (*3-DOF*) model is employed, encompassing surge, sway, and yaw motions. The remaining degrees of freedom, namely roll, pitch, and heave, are neglected. This simplification is justified as the research primarily focuses on the planar path-following problem, under the assumption that the hull design ensures sufficient hydrostatic stability.

As depicted in Figure 1, the motion of the USV is described using two coordinate frames: the earth-fixed inertial frame {*E*} and the body-fixed frame {*B*}.

The Earth-fixed frame *{E}* ($O_E X_E Y_E$) his inertial frame is utilized to determine the absolute position (*x, y*) the trajectory, and the heading angle ($\psi$) of the vessel.

The Body-fixed frame *{B}*($O_B x_b y_b$), This moving frame is attached to the USV hull and is utilized to describe the linear velocities *(u, v)* and the angular velocity *(r)*.

The kinematic equations describing the relationship between these two coordinate frames are expressed as follows:

$$\dot{\boldsymbol{\eta}} = \boldsymbol{J}(\psi)\boldsymbol{\nu} \quad (1)$$

Where:

$\boldsymbol{\eta} = [x, y, \psi]^T$ enotes the position and orientation vector with respect to the Earth-fixed frame *{E}*.

$\boldsymbol{\nu} = [u,v,r]^T$ represents the velocity vector expressed in the Body-fixed frame *{B}*.

$\boldsymbol{J}(\psi)$ is the coordinate transformation matrix (Rotation Matrix), defined as:

$$\boldsymbol{J}(\psi) = \begin{bmatrix} cos\,\psi & -sin\psi & 0 \\ sin\psi & cos\,\psi & 0 \\ 0 & 0 & 1 \end{bmatrix} \quad (2)$$

**Nonlinear Dynamic Equations:**

Based on the Newton-Euler formulation and the theoretical framework established by Fossen [5], the dynamic equations of the USV are expressed in matrix form as follows:

$$\boldsymbol{M}\dot{\nu} + \boldsymbol{C}(\nu)\boldsymbol{\nu} + \boldsymbol{D}(\boldsymbol{\nu})\boldsymbol{\nu} = \boldsymbol{\tau}+\boldsymbol{\tau}_{env} \quad (3)$$

Where:

$\boldsymbol{M} \in \{R\}^{3x3}$: Mass and Added mass matrix.

$\boldsymbol{C(\nu)}$ $\in\{R\}^{3x3}$: Coriolis and Centripetal matrix.

$\boldsymbol{D(\nu)}$ $\in\{R\}^{3x3}$: is the hydrodynamic damping matrix, which incorporates both linear and nonlinear terms.

$\boldsymbol{\tau} = [\ \tau_u,\ 0,\ \tau_r]^T$: denotes the control input vector, consisting of the surge force and yaw moment generated by the main propeller and rudder system. It is important to note that the USV is an under-actuated system (lacking

a transverse thruster); consequently, the control force in the sway direction is zero ($\tau_v = 0$).

$\boldsymbol{\tau}_{env}$: represents the environmental disturbance vector, accounting for the effects of wind, waves, and ocean currents.

**Path Following Error Dynamics:**

To facilitate the implementation of LQR/LQI optimal control algorithms, the nonlinear dynamic model must be linearized around an operating point or transformed into a state-space error model. Consequently, the fundamental control objective is to minimize the following two primary error components:

**Cross-track error ($y_e$):** The perpendicular distance from the USV's center of gravity (CoG) to the desired reference path.

**Heading error ($\psi_e$):** The angular deviation between the actual vessel heading and the tangential angle of the reference path.

Under the assumption that the USV maintains a constant surge velocity ($u = Ud$) and the heading error is sufficiently small (allowing for the small-angle approximation ($sin\psi_e \approx \psi_e$), the linearized state-space equation governing the path-following error dynamics is expressed as:

$$\dot{X} = \boldsymbol{A}X + \boldsymbol{B}U + \boldsymbol{E}d_{env} \quad (4)$$

Where:

State vector, defined as: $\boldsymbol{X} = [\, y_e, \dot{y_e}, \psi_e, \dot{\psi_e}]^T$.

Control input: $U = \delta$ (rudder angle). In Equation (4), **E** represents the disturbance input matrix, which maps the external environmental forces and moments $\mathbf{d_{env}}$ (wind, waves, and currents) into the state-space derivative. This matrix defines how these disturbances directly affect the cross-track error, heading error, and their respective rates

The system matrix $\boldsymbol{A}$ and the input matrix $\boldsymbol{B}$ are dependent on the vessel's hydrodynamic parameters and the surge velocity $U_d$.

$$\boldsymbol{A} = \begin{bmatrix} 0 & 1 & 0 & 0 \\ 0 & a_{22} & a_{23} & a_{24} \\ 0 & 0 & 0 & 1 \\ 0 & a_{42} & a_{43} & a_{44} \end{bmatrix}, \boldsymbol{B} = \begin{bmatrix} 0 \\ b_2 \\ 0 \\ b_4 \end{bmatrix}$$

$d_{env}$: the environmental disturbance components acting on the system.

This state-space model serves as the basis for the design of the Fuzzy-LQI controller in the subsequent section, with the primary objective of driving the state vector $X \rightarrow 0$ as $t \rightarrow \infty$ .

## 3. FUZZY-LQI CONTROLLER DESIGN

### 3.1. Control System Architecture

Building upon the dynamic analysis presented in Section 2, the control system is designed using a hybrid control structure, as depicted in Figure 2. This architecture comprises two distinct control loops: the inner loop utilizes an LQI optimal controller to ensure system stability and precise path tracking, while the outer loop employs a Fuzzy Supervisor to perform adaptive parameter tuning.

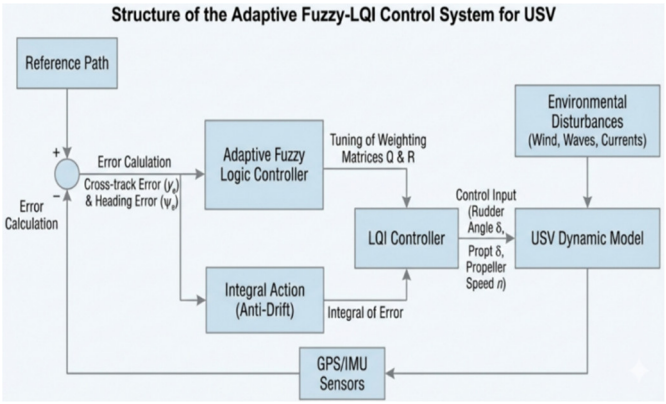


Figure 2. Block diagram of the adaptive Fuzzy-LQI control system for the USV

The proposed closed-loop control architecture operates synergistically to ensure precise path following through the following core components: Error Calculation: Computes the instantaneous cross-track error ($y_e$) and heading error ( $\psi_e$) by comparing the USV's measured state (via GPS/IMU) with the reference trajectory.

Integral Action (Anti-Drift): Augments the traditional LQR framework by integrating tracking errors over time. This generates a continuous compensatory control effort to eliminate steady-state drift induced by persistent environmental disturbances.

Fuzzy Logic Controller: Serves as the adaptive tuning mechanism for the weighting matrices ($Q$ and $R$). During large trajectory deviations, it increases $Q$ to prioritize rapid tracking convergence. Conversely, when errors are minimal, it decreases $Q$ and increases $R$ to optimize energy efficiency, ensure smooth motion, and mitigate actuator chattering.

LQI Controller & USV Plant: The LQI unit utilizes the augmented state and Fuzzy-updated weights to compute optimal control inputs (e.g., rudder angle $\delta$ and propeller speed $n$). These signals drive the USV under stochastic environmental loads (wind, waves, and

currents), with the resulting state continuously fed back to close the loop.

### 3.2. Linear Quadratic Integral (LQI) Controller

In contrast to previous studies that relied solely on the standard LQR framework [4], this research incorporates the integral of the cross-track error into the system's state vector. The primary objective is to eliminate steady-state errors induced by low-frequency environmental disturbances (such as river currents and crosswinds) without requiring precise modeling of these external forces.

The augmented state vector is defined as:

$$\tilde{x} = \begin{bmatrix} x \\ x_I \end{bmatrix} = \begin{bmatrix} y_e \\ \dot{y}_e \\ \psi_e \\ \dot{\psi}_e \\ \int y_e dt \end{bmatrix} \quad (5)$$

Where: $x_I = \int_0^t y_e(\tau)d\tau$ the integral of the cross-track error.

The augmented state-space system is formulated as follows:

$$\dot{\tilde{x}} = \tilde{A}\tilde{x} + \tilde{B}u \quad (6)$$

The augmented system matrices are defined as:

$$\tilde{A} = \begin{bmatrix} A & 0_{4x1} \\ C_{y_e} & 0 \end{bmatrix}; \ \tilde{B} = \begin{bmatrix} B \\ 0 \end{bmatrix}$$

$C_{y_e} = [1,0,0,0]$ is the output matrix used to extract the cross-track error from the state vector. $y_e$.

The LQI design problem is formulated as finding the optimal control input $u(t)$ that minimizes the following quadratic cost function:

$$J = \int_0^\infty (\tilde{x}^T Q \tilde{x} + u^T R u)dt \quad (7)$$

Where:

$Q \geq 0$: denotes the state weighting matrix, which penalizes state deviations. A larger value of elements in $\boldsymbol{Q}$ implies that the system prioritizes path-following accuracy (minimizing tracking errors).

$R > 0$: denotes the control weighting matrix, which penalizes control effort (energy consumption). A larger value of $\boldsymbol{R}$ results in more conservative energy usage, leading to smaller rudder angles and smoother actuation.

The optimal state feedback control law is given by:

$$u(t) = -K_{LQI}\tilde{x}(t) \quad (8)$$

Vector gain $K_{LQI}$ is determined by solving the Algebraic Riccati Equation (ARE), ensuring that the closed-loop system achieves asymptotic stability based on Fossen's control theory.

### 3.3. Fuzzy Logic-based Adaptation Mechanism

The conventional LQI controller is inherently constrained by its fixed weighting matrices, $Q$ and $R$, which impose a fundamental trade-off between path-tracking precision and control energy consumption, as illustrated in Figure 3. To overcome this rigid limitation, this study introduces an adaptive mechanism utilizing a Fuzzy Inference System (FIS) to dynamically adjust the control weights in real-time based on the instantaneous cross-track error.

Figure 3 illustrates the proposed Fuzzy Logic Adaptation Mechanism for the LQI Controller, which is designed to dynamically adjust the weighting matrices of the Linear Quadratic Integral (LQI) controller in response to real-time tracking performance. The primary objective of this mechanism is to enhance robustness and adaptability under varying system dynamics and external disturbances.

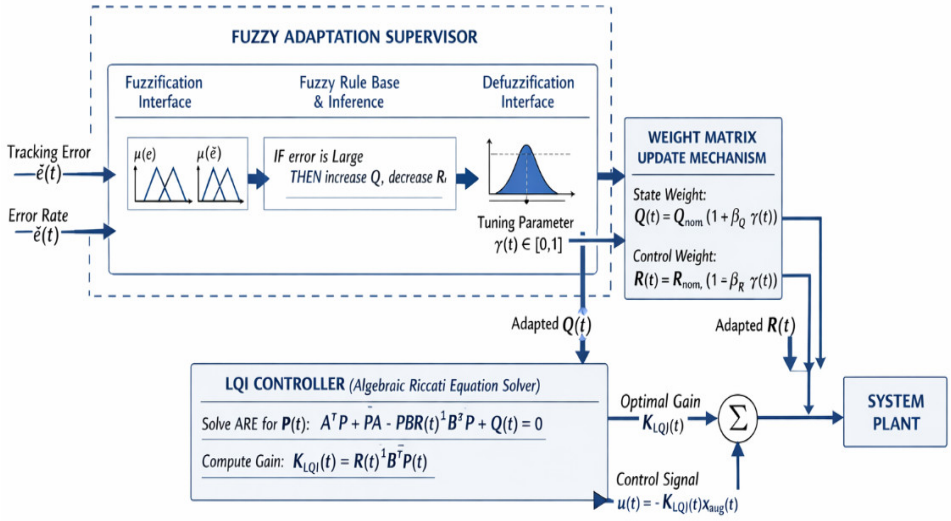


Figure 3. Fuzzy Logic Adaptation Mechanism for LQI Controller

#### Input Signals and Fuzzy Adaptation Supervisor:

The Supervisor Logic distinguishes between nominal and extreme environments by evaluating the real-time tracking performance. In a nominal environment (calm sea), where the tracking error $e(t)$ and error rate $\dot{e}(t)$, remain within small predefined thresholds, the

supervisor maintains a low $\gamma(t)$ value, effectively operating in a standard LQR mode to optimize energy efficiency. Conversely, an extreme environment is identified when large deviations or rapid error changes occur (e.g., due to strong gusts or currents); the supervisor then increases $\gamma(t)$ to activate the Fuzzy-LQI mode, prioritizing disturbance rejection and steady-state error elimination over energy saving.

The adaptation process begins with two real-time performance indicators:

The tracking error, $e(t)$, defined as the difference between the reference signal and the system output.

The error rate, $\dot{e}(t)$, representing the temporal variation of the tracking error.

These two signals are fed into the Fuzzy Adaptation Supervisor, which operates as a high-level supervisory controller. The supervisor is implemented using fuzzy logic to incorporate heuristic control knowledge and handle nonlinearities without requiring an explicit mathematical model of the uncertainty.

Within the supervisor, three sequential stages are employed:

Fuzzification Interface: The crisp input variables $e(t)$ and $\dot{e}(t)$, are transformed into fuzzy linguistic variables using predefined triangular membership functions. These membership functions, denoted as $\mu(e)$ and $\mu(\dot{e})$, typically represent qualitative levels such as *Small*, *Medium*, and *Large*.

Fuzzy Rule Base and Inference Engine: The fuzzy inference system evaluates a set of expert-defined IF–THEN rules. A representative rule is:

*IF the tracking error is Large, THEN increase the state weighting matrix Q and decrease the control weighting matrix R.*

This rule structure reflects a common control heuristic: prioritizing tracking accuracy when errors are significant, while relaxing control effort penalties.

Defuzzification Interface: The inferred fuzzy outputs are converted back into a crisp scalar value using the center-of-gravity defuzzification method. The resulting output is the tuning parameter $\gamma(t) \in [0,1]$, which quantitatively represents the required adaptation intensity.

**Weight Matrix Update Mechanism**

The tuning parameter $\gamma(t)$ is forwarded to the Weight Matrix Update Mechanism, where it is used to adjust the LQI cost function weights in real time. Specifically, the state and control weighting matrices are updated according to:

$$Q(t) = Q_{nom}(1 + \beta_Q \gamma(t)) \quad (9)$$

$$R(t) = R_{nom}(1 + \beta_R \gamma(t)) \quad (10)$$

where $Q_{nom}$ and $R_{nom}$ denote the nominal weighting matrices, and $\beta_Q$, $\beta_R$ are positive scaling factors that determine the sensitivity of the adaptation process.

This formulation ensures that:

Larger tracking errors result in a higher state penalty $Q(t)$ enforcing tighter tracking.

The control penalty $R(t)$ is reduced accordingly, allowing more aggressive control actions when necessary.

***LQI Controller and Gain Computation***

The adapted matrices $Q(t)$ and $R(t)$ are supplied to the LQI Controller, which computes the optimal feedback gain by solving the time-varying Algebraic Riccati Equation (ARE):

$$\boldsymbol{A}^T\mathbf{P}(t) + \boldsymbol{P}(t)\boldsymbol{A} - \boldsymbol{P}(t)\boldsymbol{B}\boldsymbol{R}(t)^{-1}\boldsymbol{B}^T\boldsymbol{P}(t) + \boldsymbol{Q}(t) = 0 \quad (11)$$

Based on the solution $P(t)$, the optimal LQI gain is obtained as:

$$\boldsymbol{K}_{LQI}(t) = \boldsymbol{R}(t)^{-1}\boldsymbol{B}^T\boldsymbol{P}(t) \quad (12)$$

This adaptive gain reflects the current system performance and automatically balances tracking accuracy and control effort.

**Control Law and Closed-Loop Operation**

The computed gain $K_{LQI}(t)$ is applied to the **augmented state vector** $x_{aug}(t)$, which includes both the system states and the integral of the tracking error. The resulting control law is given by:

$$u(t) = -K_{LQI}(t)x_{aug}(t) \quad (13)$$

The control signal $u(t)$ is then applied to the system plant, whose output is fed back to generate updated tracking error signals. This closed-loop structure enables continuous online adaptation.

**Overall Operating Principle**

In summary, the proposed architecture combines fuzzy logic supervision with optimal control theory. The fuzzy supervisor provides qualitative, human-like decision-making to adapt the LQI weighting matrices, while the LQI controller ensures optimal performance based on a rigorous mathematical framework. This hybrid approach significantly improves robustness, adaptability,

and control performance in the presence of model uncertainties and time-varying disturbances.

This mechanism overcomes the 'rigidity' drawback of traditional optimal controllers as pointed out by Wang and Pan [4], while simultaneously achieving an optimal balance between two conflicting objectives: Tracking Quality (Accuracy) and Energy Efficiency.

To implement the presented theoretical framework, the control algorithm is structured as a real-time computational loop. This process ensures synchronous coordination among sensor acquisition, fuzzy-based parameter adaptation, and the computation of the optimal steering law. The detailed execution sequence is depicted in the flowchart in Figure 4.

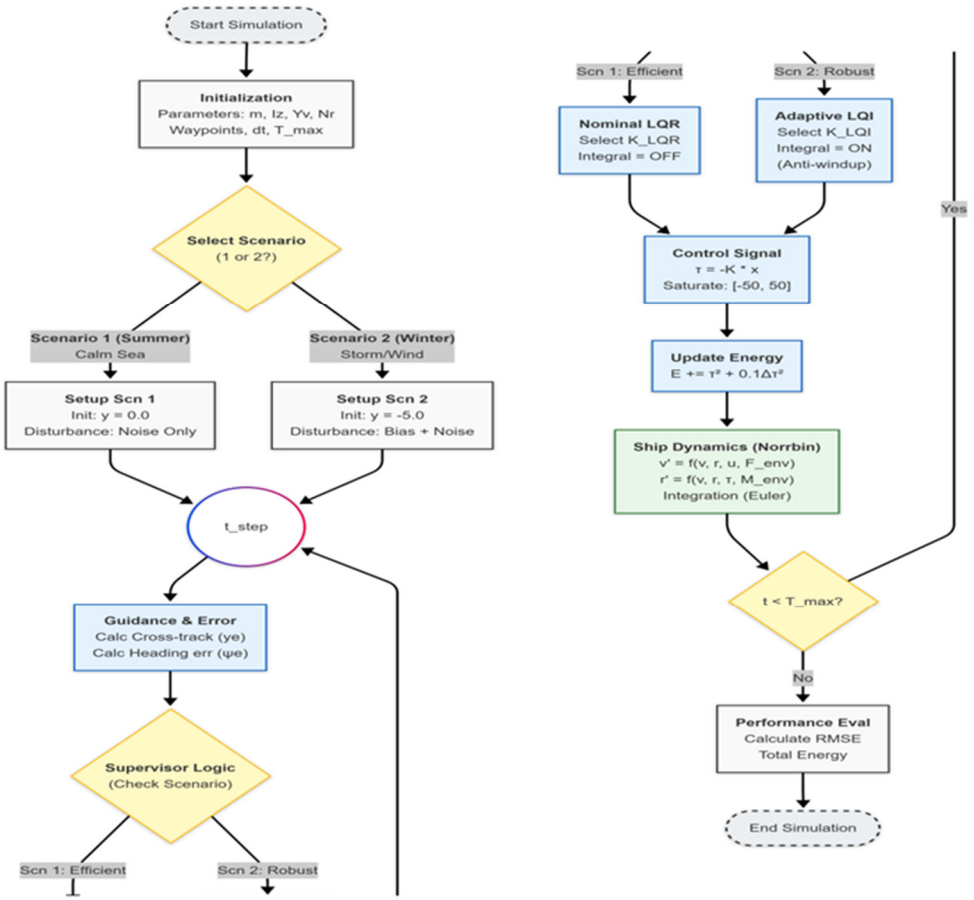


Figure 4. Flowchart of the Fuzzy-LQI adaptive control algorithm

As illustrated in the flowchart, the proposed algorithm is executed through **three well-defined processing phases** to ensure the objectivity and consistency of the simulation outcomes.

**Initialization Phase:** In this phase, the vessel's dynamic parameters, including the mass mmm and the yaw moment of inertia Izl_zlz, together with the predefined navigation waypoints, are initialized. Particular attention is given to the specification of the **initial conditions**, which are configured in accordance with the considered operational **scenarios**. Specifically, the **initial lateral offset** is set to $y_{init} = 0$ for the *Summer* scenario, corresponding to a nominal steady-state cruising condition, whereas for the *Winter* scenario it is set to $y_{init} = -5.0$, representing an initial vessel displacement induced by severe **environmental disturbances** at the onset of the simulation.

**Supervisory Control Loop:** At each discrete sampling instant with a sampling period of $dt = 0.05s$, the supervisory controller evaluates the active **scenario** and accordingly selects the appropriate control strategy.

**Execution and Evaluation:** The computed control input τ\tauτ is first passed through a physical saturation block with limits of $\pm 50Nm$ before being applied to the Norrbin vessel dynamic model. The overall system performance is continuously monitored using a generalized energy-based objective function defined as:

$$E = \sum(\tau^2 + 0.1\Delta\tau^2)dt \quad (14)$$

where the term $0.1\Delta\tau^2$ is incorporated to penalize high-frequency control oscillations, thereby protecting the actuator and improving control smoothness.

## 4. SIMULATION RESULTS AND DISCUSSION

To validate the effectiveness and superiority of the proposed Fuzzy-LQI control algorithm, a numerical simulation framework was developed using the Python 3.8 programming language. The stochastic differential equations (SDEs) governing the vessel dynamics were solved using the SciPy library with the ODEINT numerical integration scheme. A fixed time step of $\Delta t = 0.1s$ was employed, while double-precision (64-bit) floating-point arithmetic was used to ensure numerical accuracy and stability throughout the simulations.

### 4.1. Simulation Environment Setup

#### *4.1.1. USV Model Parameters*

In this study, the controlled plant is selected as the standard Cybership II model vessel (1:70 scale), with hydrodynamic parameters defined according to Fossen [5]. To facilitate the design of the trajectory-tracking controller while preserving the nonlinear characteristics of the system, the vessel dynamics are represented using the Norrbin mathematical structure. The physical parameters and hydrodynamic damping coefficients employed to construct the system state matrix $\bar{A}$ and the input matrix $\bar{B}$ are summarized in Table 1.

Table 1. Technical parameters of the USV model (Cybership II) [5]

| Parameter | Symbol | Value | Unit |
|---|---|---|---|
| Vessel mass | $m$ | 23.8 | kg |
| Hull length | $L$ | 1.255 | m |
| Yaw moment of inertia | $I_z$ | 1.76 | kg.m$^2$ |
| Linear damping coefficient (Surge) | $X_u$ | -0.72 | kg/s |
| Linear damping coefficient (Sway) | $Y_u$ | -0.88 | kg/s |
| Linear damping coefficient (Yaw) | $N_r$ | -1.90 | kg.m$^2$/s |

#### *4.1.2. Mathematical Modeling of Environmental Disturbances*

To realistically represent practical operating conditions, external environmental disturbances are modeled as a resultant **force–moment vector** acting on the vessel:

$$\tau_{env} = \tau_{wind} + \tau_{wave} + \tau_{current} \quad (15)$$

The input parameters for this environmental model are extracted from statistical meteorological and oceanographic data for the Quang Ninh coastal waters (e.g., Ha Long Bay), in accordance with the Vietnamese standard QCVN 02:2022/BXD [11].

Since the primary focus of this study is the synthesis and evaluation of the control algorithm, detailed hydrodynamic and aerodynamic equations are omitted for brevity. Instead, standard empirical and stochastic models are employed to simulate the individual disturbance components:

Wave Model ($\tau_{wave}$) The sea surface state is reconstructed using the JONSWAP (Joint North Sea Wave Project) wave energy spectrum. This model is highly appropriate for nearshore marine environments characterized by limited water depth and fetch conditions.

Wind Model ($\tau_{wind}$): Wind-induced forces and moments are computed based on the widely adopted Isherwood (1972) aerodynamic model. The resultant wind velocity incorporates both a constant mean component and a stochastic gust component (modeled as Gaussian white noise) to rigorously assess the sensitivity and robustness of the proposed control scheme.

Current Model ( $\tau_{current}$): To accurately capture the time-varying characteristics of natural ocean currents in real-time, the 2D current velocity is modeled as a first-order Gauss-Markov stochastic process.

#### *4.1.3. Configuration of the Simulation Environmental Parameters*

To systematically evaluate the robustness of the proposed control algorithm, two testing scenarios are constructed based on meteorological and oceanographic data from the Quang Ninh coastal region [11]. Rather than relying on purely random assumptions, these scenarios apply explicit boundary conditions and disturbances to stress-test the system, as detailed in Table 2.

Scenario 1 (Standard Operating - Summer): Represents calm sea conditions with low-amplitude Gaussian noise and zero initial offset ($y_{init} = 0$). This serves as the baseline to assess the controller's trajectory tracking accuracy and energy efficiency.

Scenario 2 (Extreme Operating - Winter): Represents severe storm-like conditions. It subjects the system to a dominant constant lateral drift force of 4.0N deliberately chosen to exceed the compensation limits of conventional linear LQR coupled with induced yaw moments. Furthermore, the vessel is initialized with a significant lateral offset ($y_{init} = -5.0m$) to simulate a worst-case loss of directional control. The objective is to verify the algorithm's capability for rapid trajectory recovery and steady-state error rejection.

Table 2. Quantitative parameters of the simulation environment (based on data from [11])

| Parameter | Scenario 1 (Nominal) | Scenario 2 (Extreme) | Physical interpretation |
|---|---|---|---|
| Lateral wind/wave force, $F_y$ (N) | $0.2\cos(0.5t)$ | $4.0+1.5\sin(0.3t)$ | Constant bias force of **4.0N** represents dominant drift-inducing disturbance under strong Northeast monsoon conditions |
| Yaw moment, $M_z$ (Nm) | $0.1\sin(0.5t)$ | $0.5F_y$ | Coupled yaw disturbance induced by asymmetric wind and wave loading, causing heading deviation |

| | | | |
|---|---|---|---|
| Initial lateral position $y_{init}$ (m) | *0.0* | *−5.0* | Worst-case initial offset simulating loss of directional control under severe sea state |
| Test objective | Control smoothness | Position accuracy *(e⟶0)* | Evaluation of trajectory recovery capability and steady-state error rejection |

#### *4.1.4. Reference Trajectory and Benchmarking Methodology*

To comprehensively evaluate the proposed Fuzzy-LQI controller against a conventional fixed-weight LQR, the simulation employs a U-shaped reference trajectory defined by sequential waypoints: $WP_1(0,0) \rightarrow WP_2(100,0) \rightarrow WP_3(100,50) \rightarrow WP_4(0,50)$. This geometric configuration rigorously tests both steady-state tracking accuracy on straight segments and transient performance during sharp $90^0$ turns. To rigorously assess the transient recovery capability, the vessel is initialized at $(x_0, y_0) = (0, -5)$ m with a heading of $\psi_0 = 0^0$. This initial 5-meter lateral offset enforces an immediate, aggressive line-capturing maneuver at $t = 0$.

The quantitative benchmarking between the controllers is conducted based on two primary performance indices: the Root Mean Square Error (RMSE) to measure path-following accuracy, and the total steering energy consumption to evaluate actuation efficiency and control effort.

### 4.2. Analysis of Simulation Results

Table 3. Summary of Control Performance Comparison between LQR and Fuzzy-LQI

| Cenario | Controller | RMSE (m) | Total Energy Consumption (E) | System Behavior Assessment |
|---|---|---|---|---|
| Scenario 1 (Summer – Calm Sea) | LQR (Baseline) | 0.667 | 17.4 | Accurate path following with low energy expenditure |
| | Fuzzy-LQI (Proposed) | 0.667 | 17.4 | Performance equivalent to baseline LQR |
| Scenario 2 (Winter - Severe Disturbances) | LQR (Baseline) | 15.229 | 15.229 | Loss of regulation due to steady-state drift |
| | Fuzzy-LQI (Proposed) | 1.168 | 1294.6 | Stable trajectory recovery under strong disturbances |

The quantitative simulation results are systematically summarized in Table 3. The data highlight a clear performance distinction between the conventional fixed-gain LQR and the proposed adaptive Fuzzy-LQI controller across contrasting environmental conditions. While both control strategies exhibit identical, highly efficient tracking performance under nominal conditions (Scenario 1), the proposed Fuzzy-LQI demonstrates superior robustness, trajectory recovery, and steady-state drift rejection when subjected to extreme marine disturbances (Scenario 2).

#### *4.2.1. Trajectory Response and Tracking Error Analysis*

The simulated trajectory responses and corresponding tracking errors are illustrated in Fig. 5. As shown in Figure 5 (a,b,c,d), the blue dashed line represents the baseline LQR controller, while the solid red line denotes the proposed Fuzzy-LQI controller. The points A, B, C, and D indicate the sequential reference waypoints. In this nominal scenario, the two trajectories overlap, confirming the supervisor's selection of the energy-efficient mode

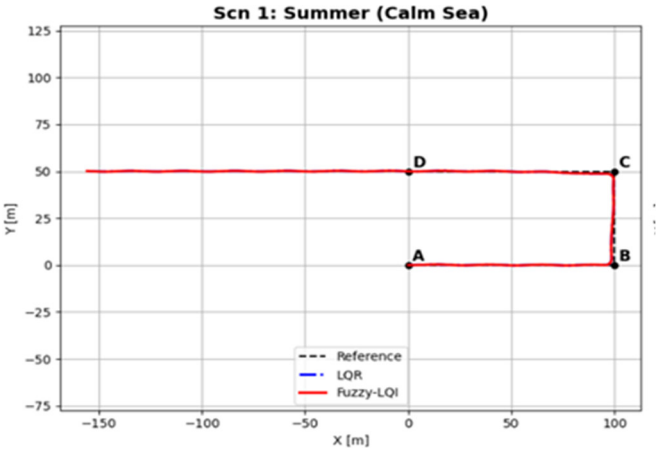


a)

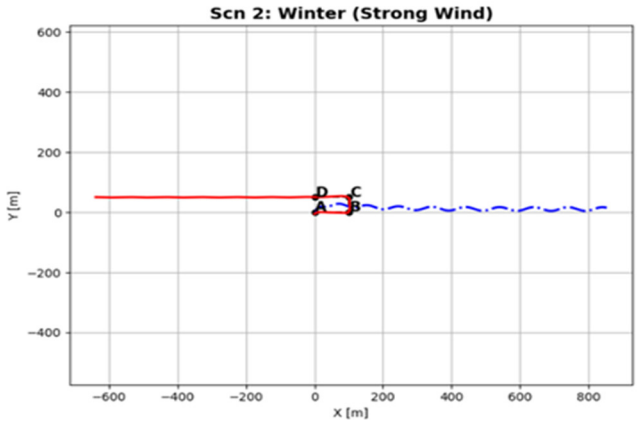


b)

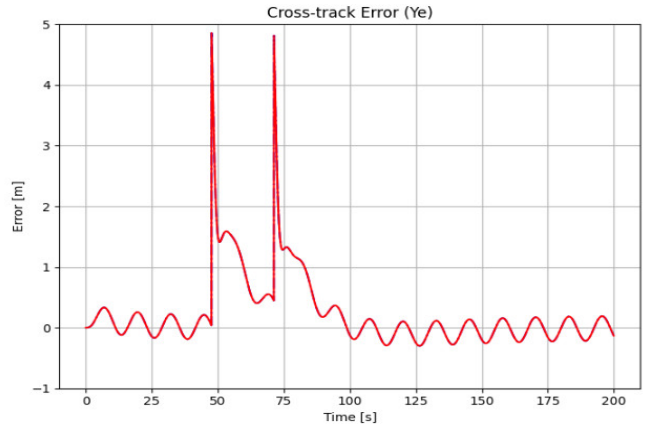


c)

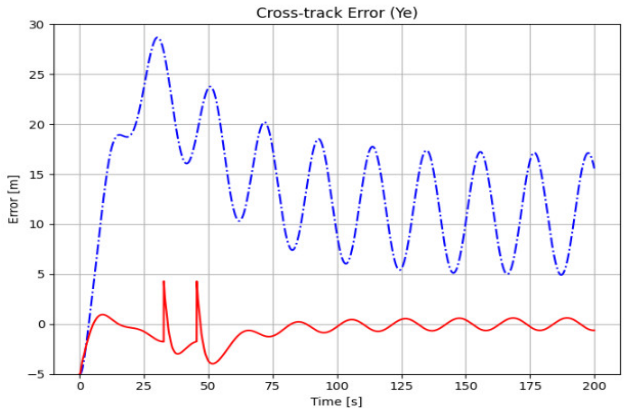


d)

Figure 5. Trajectory tracking performance and lateral error responses under nominal and extreme environmental conditions

Figure 5 presents a comparative visualization of the system output responses under the two operating scenarios. Specifically, Figure 5(a) and Figure 5(b) depict the actual vessel trajectories with respect to the reference path for Scenario 1 (nominal summer conditions) and Scenario 2 (extreme winter disturbances), respectively. Meanwhile, Figure 5(c) and Figure 5(d) show the corresponding lateral trajectory tracking errors $y_e$ as functions of time.

Scenario 1 (Nominal Summer Conditions): Under Scenario 1, the trajectory response of the proposed Fuzzy-LQI controller (solid red line) completely overlaps with that of the baseline LQR controller (blue dashed line), as illustrated in Figure 5(a). Both controllers accurately track the predefined waypoints A, B, C, and D, with negligible oscillations and a maximum lateral deviation of less than 0.7m.

This result confirms that, under mild Gaussian white noise disturbances, the supervisory mechanism correctly selects the nominal LQR mode, enabling smooth system operation without inducing overshoot or unnecessary control actions.

A similar observation can be made from the lateral tracking error responses shown in Figure 5(c). The error trajectories of the Fuzzy-LQI (red) and LQR (blue dashed) controllers are almost indistinguishable. At the heading transition points (around t = 50s and t = 75s), the peak tracking error briefly reaches approximately 4.8m before rapidly converging back to zero. This behavior verifies that, under light disturbances, the supervisory controller maintains the nominal control strategy while preserving tracking smoothness equivalent to that of the conventional LQR controller.

Scenario 2 (Extreme Winter Conditions): The structural differences between the two control strategies become most evident in the lateral tracking error responses under Scenario 2, as shown in Figure 5(d).

Failure of the LQR controller (blue dashed line): Due to the absence of an integral action capable of compensating for the constant lateral wind force of 4.0N, the standard LQR controller fails to restore the vessel to the reference trajectory. As observed in Figure 5(d), the lateral error $y_e$ does not converge but instead exhibits large-amplitude sinusoidal oscillations, ranging approximately from 5m to 28m, with a mean offset of about 15m. This phenomenon indicates an oscillatory drift, where the vessel remains persistently displaced from the desired path under sustained environmental bias.

Effectiveness of the proposed Fuzzy-LQI controller (solid red line): In contrast, despite an unfavorable initial lateral offset ($y_{init}$ = −5.0m), the Fuzzy-LQI-controlled system rapidly suppresses the tracking error within the first *20* seconds. Even under continuous storm-like disturbances, the lateral error remains stably bounded around zero, demonstrating the controller's ability to reject persistent disturbances and recover the desired trajectory through adaptive supervisory integral action.

#### *4.2.2. Control Effort and Energy Consumption Analysis*

The time responses of the control input (steering torque $\tau$) are illustrated in Figure 6(a) and Figure 6(b), providing a direct representation of the control effort required to maintain system stability and trajectory tracking performance under different operating conditions.

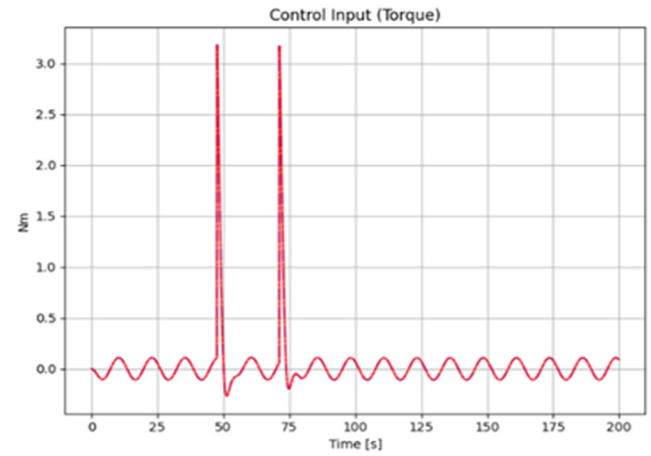


a)

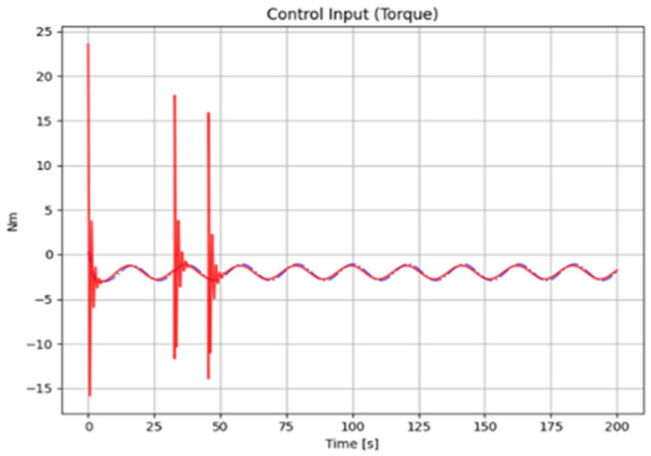


b)

Figure 6. Control torque responses τ under two simulation scenarios: (a) Scenario 1 (nominal summer conditions); (b) Scenario 2 (extreme winter conditions)

Under Nominal Operating Conditions (Scenario 1 - Figure 6(a)).

Similarity in control behavior: The control torque generated by the proposed Fuzzy-LQI controller (solid red line) perfectly coincides with that of the nominal LQR controller (blue dashed line). Both controllers maintain very low-amplitude oscillations (approximately ±0.2Nm) along straight path segments, while producing only the necessary impulsive control actions (up to 3.2Nm) at waypoint transitions.

Interpretation: This result demonstrates the effective operation of the supervisory mechanism. In the absence of significant environmental disturbances, the adaptive components are automatically suppressed, allowing the controller to revert to the nominal LQR mode. As a consequence, the system achieves smooth control behavior with minimal energy expenditure, corresponding to the lowest recorded energy consumption ($E \approx 17.4$).

Under Extreme Operating Conditions (Scenario 2 - Figure 6(b)).

The observed difference in total energy consumption between the two controllers (1294.6 vs. 918.4) can be clearly explained by analyzing the control torque responses over two distinct phases.

Initialization and Recovery Phase (0 s - 50 s): This phase represents the most critical period of system operation. For the proposed Fuzzy-LQI controller (solid red line), a substantial control effort is immediately deployed at $t = 0$ to compensate for the unfavorable initial lateral offset of −5.0m. This results in a pronounced initial control burst, with the steering torque peaking at nearly 24Nm, which is approximately eight times higher than the peak value observed under nominal conditions. Subsequently, additional high-magnitude corrective actions occur around $t$ = 35s and $t$ = 50s, forcing the vessel back toward the reference trajectory. These intensive recovery maneuvers during the first 50 seconds constitute the primary contributor to the increased total energy consumption.

In contrast, the baseline LQR controller (blue dashed line) exhibits a noticeably weaker response to the large initial deviation. The control signal lacks a decisive corrective action and remains comparatively low in amplitude, leading to an inability to counteract the strong lateral disturbance and allowing the vessel to drift away from the desired path.

Steady-State Phase ($t$ > 50s): Beyond the recovery phase, both controllers generate quasi-sinusoidal torque responses to cope with continuous wave-induced disturbances. However, the Fuzzy-LQI controller demonstrates a more proactive adjustment of torque phase and amplitude, effectively suppressing lateral error oscillations. Meanwhile, the LQR controller reacts in a largely passive manner, reflecting its limited disturbance rejection capability in the absence of integral action.

Discussion: The additional energy expenditure associated with the proposed Fuzzy-LQI controller should not be interpreted as inefficiency. Instead, it represents a necessary safety cost required to execute aggressive corrective maneuvers and restore the vessel from a hazardous off-track condition to a stable trajectory under extreme environmental disturbances.

For reproducibility and further validation, the complete simulation source code and parameter datasets are made publicly available in an open-access repository [12].

## 5. CONCLUSIONS AND FUTURE WORK

### 5.1. Conclusions

This paper has proposed and successfully validated a supervisory control strategy integrating fuzzy logic for the autonomous surface vessel Cybership II. The study primarily addresses the classical trade-off between energy optimality and robustness against environmental disturbances, which remains a critical challenge in marine control applications. Based on the quantitative simulation results, the following key conclusions can be drawn.

Adaptive capability: The supervisory mechanism demonstrates effective environmental scenario classification and control mode selection. Under nominal operating conditions (calm sea states), the system consistently maintains the nominal LQR mode, achieving a low trajectory tracking error ($RMSE \approx 0.67$m) with minimal energy consumption ($E \approx 17.4$). This performance is comparable to that of conventional optimal control strategies, confirming that the proposed framework does not degrade nominal efficiency.

Enhanced robustness: Under extreme operating conditions (storm-like disturbances with a constant lateral force of 4.0N and an unfavorable initial lateral offset of −5.0m), the proposed Fuzzy-LQI controller exhibits a clear structural advantage. While the standard LQR controller fails to reject the persistent disturbance and results in large steady-state deviations (exceeding 15m), the proposed approach rapidly restores trajectory convergence, reducing the tracking error to 1.168m, corresponding to an improvement factor of more than 13 times.

Practical effectiveness: The results further indicate that the increased energy consumption observed under severe environmental conditions (approximately 40% higher than that of the drifting LQR controller) should be interpreted as a necessary and justified cost. This additional control effort enables the generation of sufficient counteracting moments to ensure safe maneuvering and accurate trajectory tracking, highlighting the practical relevance of the proposed control strategy for real-world maritime applications.

### 5.2. Future Work

Future research will focus on three main directions. First, metaheuristic optimization techniques, such as particle swarm optimization (PSO) or genetic algorithms (GA), will be investigated to automatically tune the fuzzy rules and the weighting matrices QQQ and RRR, replacing the current trial-and-error approach. Second, the disturbance model will be extended to include more complex and time-varying environmental effects, such as stochastic currents and irregular wave conditions, to further evaluate controller robustness. Finally, the proposed control strategy will be implemented on a physical vessel platform and validated through hardware-in-the-loop (HIL) experiments, paving the way toward real-world maritime deployment.

**REFERENCES**

[1]. D. T. Le, T. T. H. Ta, N. D. Tran, "Research on the application of single-beam echo sounder technology for monitoring reservoir sedimentation in hydropower plants," *Journal of Construction Science and Technology* (IBST), 2-7, 2024. (in Vietnamese)

[2]. N. Nham, "Lecture on echo sounders: Theory and acoustic wave analysis," *Ho Chi Minh City University of Transport,* 2022. (in Vietnamese)

[3] Z. Liu, Y. Zhang, X. Yu, C. Yuan, "Unmanned surface vehicles: An overview of developments and challenges," *Annual Reviews in Control*, 41, 71-93, 2016.

[4]. W. Naeem, R. Sutton, J. Chudley, "Modelling and control of an unmanned surface vehicle for environmental monitoring," *Journal of Engineering for the Maritime Environment,* 222, 2, 111-121, 2008.

[5]. T. I. Fossen, *Handbook of Marine Craft Hydrodynamics and Motion Control*. John Wiley & Sons, Ltd., 2011.

[6]. N. Wang, X. Pan, "Robust trajectory tracking control for unmanned surface vehicles with neural network limit learning," *Neurocomputing*, 356, 197-206, 2019.

[7]. M. Abdelaal, M. Fränzle, A. Hahn, "Nonlinear model predictive control for trajectory tracking of unmanned surface vessels," *IEEE Access*, 6, 25348-25369, 2018.

[8]. V. V. Nguyen, C. N. Tran, "Research, calculation, and design of the propulsion system for an unmanned surface vehicle (USV) for hydrographic surveying," *Journal of Water Resources Science and Technology,* 60, 45-53, 2020. (in Vietnamese)

[9]. T. L. Le, M. T. Pham, "Design and manufacturing of an autonomous solar-powered water surface garbage collection boat model," *Journal of Vietnam Mechanical Engineering*, 12, 4, 88-95, 2021. (in Vietnamese)

[10]. V. T. Vu, T. H. Nguyen, "Design of a digital PID controller for ship heading keeping," *Journal of Transportation Science,* 70, 12-18, 2019. (in Vietnamese)

[11]. Ministry of Construction, *QCVN 02:2022/BXD: National technical regulation on natural condition data used in construction*. Construction Publishing House, Hanoi, Vietnam, 2022. (in Vietnamese).

[12]. L. Q. Thang, *Simulation Source Code for Fuzzy-LQI Control of Cybership II*. GitHub repository, 2025. [Online]. Available: https://github.com/lequyetthang5282-spec/CybershipII-FuzzyLQI/tree/main.